ISSN 2616-7433 Vol. 2, Issue 12: 116-122, DOI: 10.25236/FSST.2020.021217

Design of F1 Race Car Rear Wing Airfoil: Optimizing the Lift to Drag Ratio through Numerical Simulation

Zihao Zhou

Beijing National Day School, Beijing 100039, China
zihaomickey2002@163.com

ABSTRACT. *The rear wing of a Formula One race car generates both aerodynamic downforce and drag. While downforce improves cornering speed, drag impedes straight-line speed. Race car engineers have long struggled to balance downforce and drag, often sacrificing one in pursuit of the other. In this work, we address this problem by designing a constant-chord-length inverted rear wing airfoil that has an optimal lift to drag ratio. Using an elliptical airfoil as a base for modification, we examined how variations in maximum suction-side and pressure-side thickness, location of suction-side and pressure-side vertices, and leading edge-radii affected the airfoil's lift-drag ratio. We computed the lift-drag ratio and the flow field of over 40 test airfoils through finite-element numerical simulation using ANSYS FLUENT. By comparing these simulation results, we identified distinct design trends and produced an airfoil with a high lift-drag ratio of 62 at the average speed of formula one cars. This high-performance airfoil has the potential to be effectively applied to race cars, and even to regular cars to enhance grip and improve driving safety without sacrificing fuel economy.*

KEYWORDS: *F1 rear wing, Airfoil, Lift-drag ratio, Optimization, CFD*

1. Introduction

Formula One race cars can reach top speed of over 330 kilometers per hour and maintain an average speed of about 200km/h during the entire race. At this speed level, aerodynamic forces exert a prominent influence on the cars' performance. All Formula One cars use inverted airfoils to generate aerodynamic downforce, adding normal load on the 4 tires, thereby increasing the maximum static friction they can withstand. More friction means better grip and higher speed through the corners. However, inverted airfoils also generate drag, which slows the car down in the straight lines. For decades, race car engineers have struggled to find a balance between downforce and drag, often having to sacrifice one in pursuit of the other. Many previous airfoil researches were focused on improving the lift and reducing drag, and there are currently a wide variety of high-lift airfoil designs and low-drag airfoil designs published in open source literature, but most of these designs either focus exclusively on enhancing lift or exclusively on reducing drag, not fully considering the close correlation between lift and drag: higher lift almost always leads to greater drag. Few published studies have addressed the balance of lift and drag, Additionally, these few studies were limited to small modifications of well-known existing airfoil designs, providing only partial insights into the more generalizable principles and methods that can be applied to the design of new airfoils.[1-4] Another limitation concerning published airfoil research is that the focus of this research concerns only airplane and wind turbine airfoils; the design of inverted airfoils in high-performance automobiles is rarely considered. We aim to address the lift-drag trade off in race car wings by designing a constant-chord-length F1 rear wing airfoil that has an optimal lift to drag ratio. This style of design provides the best rational compromise between downforce and drag, enabling the car to attain a good balance between cornering stability and straight-line speed. We used a generic elliptical airfoil as a base for modification and examined how variations in several geometric characteristics affect the airfoil's lift-drag ratio. We compared the results and summarized distinct trends which were used to optimize the lift-drag ratio.

2. Methodology

2.1 Definition and Control of Variables

(1) Definition of Variables: The independent variables of this study were the maximum thicknesses of the suction side and pressure side curve, the locations (coordinates) of the suction side and pressure side vertices, and the leading-edge radius. The dependent variable was value of the lift-drag ratio.

ISSN 2616-7433 Vol. 2, Issue 12: 116-122, DOI: 10.25236/FSST.2020.021217

(2) Constants: The chord length of the airfoil was held at a constant 35 cm as mandated by the 2020 FIA Formula One Technical Regulations. The free stream air speed was set to be a constant 50 m/s-the average speed of Formula Cars during a full Grand Prix Race.

(3) Control of Variables: A control-of-variables method was employed in the study. The 3 independent variables were studied one at a time. The values of each independent variable were altered while holding the other two constant and the resultant changes in lift-drag ratio were recorded.

2.2 Geometry Modelling

Most airfoil profiles tested in this study were modified from ellipses. Using the Control Point Curve Editing Code in Rhinoceros 3D industrial modelling software, we inserted three controls points into the vertex and the two end points of an ellipse. Then, the y- and x-coordinates of the vertex control point were independently altered to adjust the maximum suction side thickness and the location of the suction side vertex along the chord. Meanwhile, the end point coordinates were held constant to maintain a constant chord length. The suction side curves generated through this process are shown in Fig. 1. The airfoils in the same row have the same suction side thickness but different vertex location, while airfoils in the same column have the same vertex location but different suction side thickness.

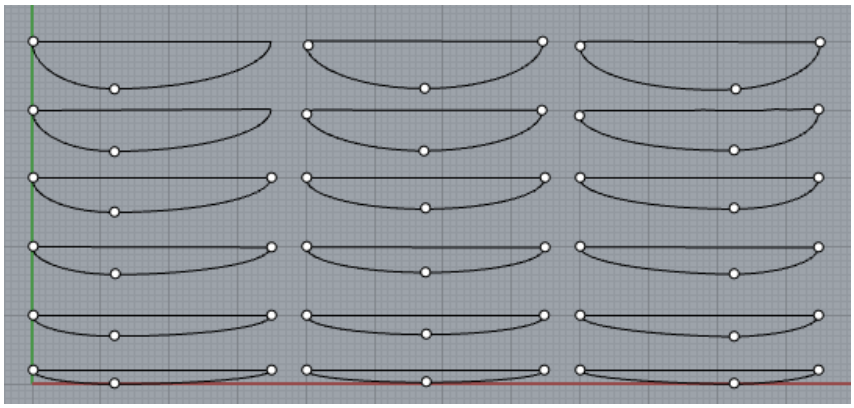

Fig.1 Suction side Curves Generated through Control-Point Editing

The same process was repeated with the pressure side curve, and fillets were added to join the suction and pressure sides. As shown in Fig.2, these airfoils employed concave pressure side curves to generate higher lift[5]. All airfoils were later imported to ANSYS FLUENT for flow field simulation.

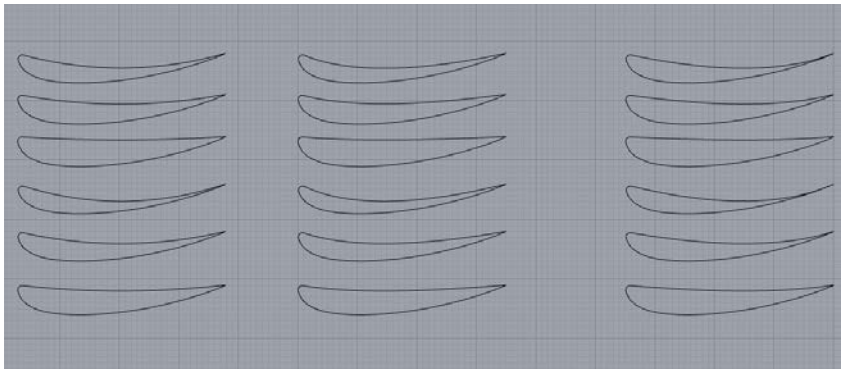

Fig.2 Pressure side Curves Generated through Control-Point Editing

The three control points we used were sufficient to model the geometric characteristics we were interested in investigating. Using a minimum number of control points, we were able to minimize the involvement of any potential confounding variables that may blur our focus on only the maximum thickness and its location.

ISSN 2616-7433 Vol. 2, Issue 12: 116-122, DOI: 10.25236/FSST.2020.021217

2.3 Simulation Methodology

ANSYS FLUENT was used to carry out numerical simulations of the flow field around the test airfoils. Prior to calculation, the test airfoils were placed inside virtual wind tunnels whose length and width were respectively 100-fold greater than the chord length and thickness of the airfoil; the large size of the virtual tunnel minimizes the influence of tunnel walls on the flow field around the airfoil. Unstructured triangular mesh was generated inside the wind tunnel fluid domain, with finer mesh units near the airfoil edge.

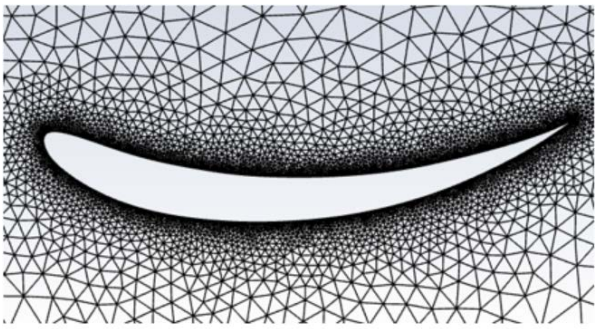

Fig.3 Mesh NEAR the Airfoil

The mesh file was imported to FLUENT and the *k-epsilon* viscous model and *SIMPLEC* solution method were employed to simulate a steady-state flow field over the airfoils. The k-epsilon model has previously been shown to generate reliable results for two-dimensional flow field simulations. [6] Inlet airspeed was set to 50 m/s. *Grid convergence test* was conducted and meshes were made fine enough for calculations to be meaningful. After convergence was reached, the calculated lift-drag ratio values were recorded. In addition, pressure and velocity contours, as well as velocity vector diagrams were also recorded.

2.4 Study Procedure

This study has two main components: test studies and optimization. While test studies are relatively rough studies conducted to observe general trends, optimization is focused on investigating in more detail the range of variables that produced desired outcomes in test studies. During test studies, airfoils with suction side vertices located at 33% (1/3) chord length, 67% (2/3) chord length, and 50% chord length (1/2) were examined. These three percentile values were chosen to represent vertex location in front of, behind, and at the center of the chord. For each location, six airfoils with relative thickness of 6%, 9%, 11%, 14%, 17%, and 20% were tested. All test airfoils incorporated a flat pressure side curve. A total of 18 airfoils were studied and the results were analyzed. During optimization, more detailed investigations were conducted in the range of variables that produced desired outcomes: Suction side vertex locations at 25% (1/4), 37% (7/19), and 40% (2/5) chord length and pressure side vertex location at 56% (5/9), 63% (5/8), and 75% (3/4) chord length were tested. Thickness was adjusted on finer scale in an attempt to yield more improvements. Various leading-edge radii were also tested, and the best-performing one was adopted. Finally, small refinements were further applied on the best-performing airfoil identified through previous steps based on the physics of its flow field.

3. Results and Development

3.1 Results of Test Studies

We found that airfoils with suction side vertices located in front of 50% chord length generated noticeably higher lift-drag ratios than those whose suction side vertices are located further behind. The mean lift-drag ratio of airfoils with suction side vertex at 33% chord length was 30.8, which is 30% larger than the mean lift-drag ratio of airfoils with suction side vertex at 50% chord length and 41% larger than the mean lift-drag ratio of airfoils with suction side vertex at 67% chord length. In addition, as shown in Fig.4, for EACH relative thickness we examined, the airfoil with suction side vertex at 33% chord length had a distinctly higher lift-drag ratio than the other two airfoils whose suction side vertices were located further behind. This consistent trend suggests that airfoils with suction side vertex located before the center of the chord generally produce higher lift-drag ratios,

ISSN 2616-7433 Vol. 2, Issue 12: 116-122, DOI: 10.25236/FSST.2020.021217

even though statistical significance cannot be concluded due to limited sample size. Meanwhile, the lift-drag ratio remains relatively stable as relative thickness varies between 6% and 14%, but begins to drop rapidly as relative thickness exceeds 14 %, primarily due to stall.

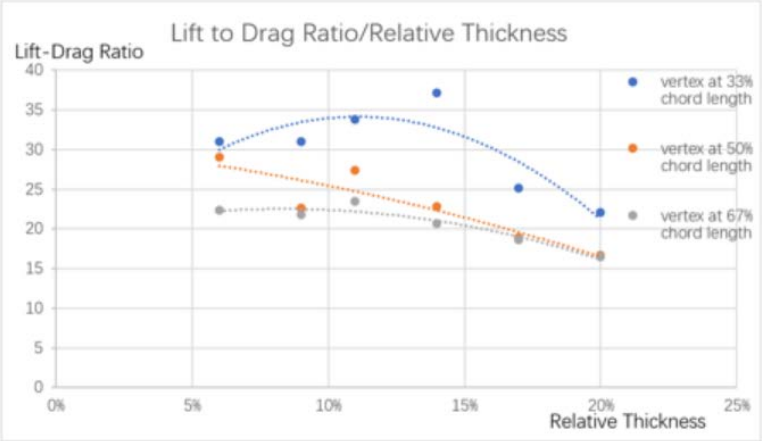

Fig. 4 Experimental relationship between lift-drag ratio and relative thickness at different suction side vertex locations

In addition, we found a strong quadratic relationship between the maximum pressure side thickness and the lift-drag ratio, with a coefficient of determination larger than 0.95. (Fig.5) The lift-drag ratio was lowest when the relative thickness was between 3% and 5%, while distinctly higher lift-drag ratios were obtained by either reducing the relative thickness to below 2% or by increasing it to above 6%. The lift-drag ratio was particularly high at a maximum relative thickness of 8.5%. Furthermore, higher lift-drag ratios were observed for airfoils whose pressure side vertices were located behind 50% chord length. Airfoils with pressure side vertex at 67% produced a mean lift-drag ratio that was 8% larger than that produced by airfoils with pressure side vertex at 33%.

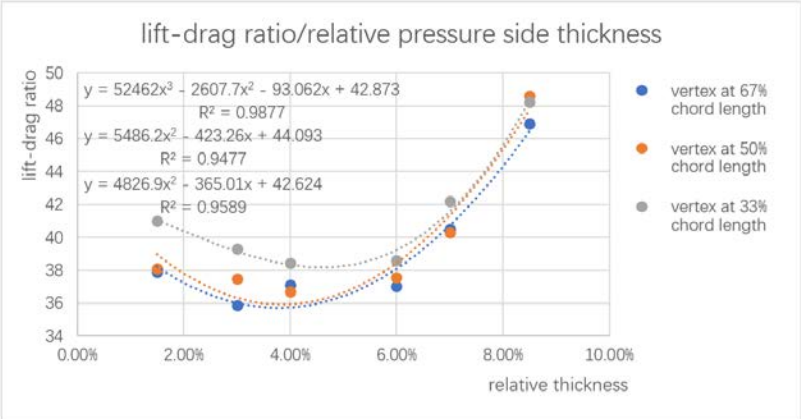

Fig.5 Experimental Relationship between Lift-Drag Ratio and Relative Thickness At Different Pressure side Vertex Locations

According to the results discussed above, we determined that airfoils with suction side vertex located in front of 50% chord length, relative suction side thickness below 15%, pressure side vertex located behind 50% chord length, and relative pressure side thickness above 8% produced the highest lift-drag ratio for Reynolds number close to 10^6. The best-performing airfoil in our test studies had a suction side vertex at 33% chord length, pressure side vertex at 67%, suction side thickness at 14%, and pressure side thickness at 8.5%. This combination produced a lift-drag ratio of 48. The flow field for this airfoil is displayed in Fig.6.

ISSN 2616-7433 Vol. 2, Issue 12: 116-122, DOI: 10.25236/FSST.2020.021217

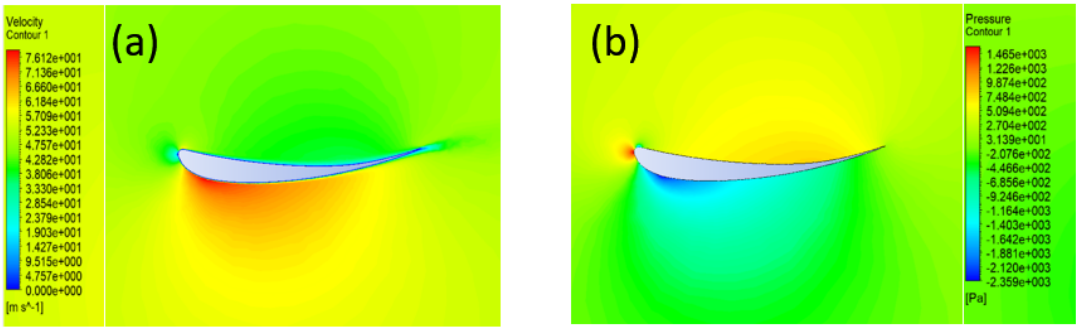

Fig.6 (a)Velocity Contour of the Best Performing Airfoil in Test Studies (B) Pressure Contour of This Airfoil

3.2 Optimization Results

Based on our results that show the range of vertex location and maximum thickness that produced high lift-drag ratios, we further investigated what values within this range generated optimal results. Using the best-performing airfoil previously identified as a base for modification, we tentatively adjusted its pressure side vertex location to 56% (5/9), 63% (5/8), and 75% (3/4), its chord length and suction side vertex location to 25% (1/4), 37% (7/19), and 40%(2/5)chord length. We added additional control points to each curve and adjusted them to make the curves smoother. We found that a 40% chord-length suction-side vertex and a 56% pressure-side vertex together yielded the largest improvement, raising the lift-drag ratio from 48 to 54.(Tab.1) It is clear that the revised profile generated a larger region of low pressure under the suction side and a larger region of high pressure on the pressure side (Fig. 6 and Fig. 7), increasing the overall lift produced. Additionally, the pressure increase behind the suction peak becomes less abrupt, delaying boundary layer separation, reducing the viscous drag.

Table 1 Data of Optimization

Pressure side vertex location	□□	□□	□□/□□
56%	1.12	0.021	51
63%	1.10	0.025	44
75%	1.39	0.028	49
67%	1.12	0.023	48
Suction side vertex location	□□	□□	□□/□□
25%	1.12	0.021	53
37%	1.13	0.023	49
40%	1.14	0.021	54
33%	1.12	0.023	48

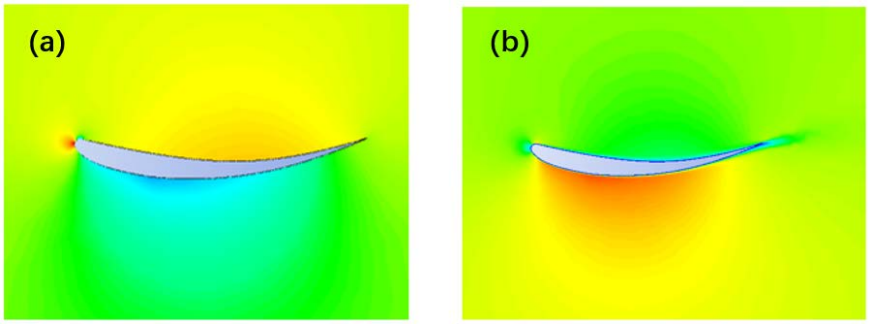

Fig.7 (a)Velocity Contour of Optimized Airfoil (B) Pressure Contour of Optimized Airfoil

To further eliminate the small amount of flow separation and loss of low pressure near the trailing edge, we tentatively reduced the maximum suction side thickness by various percentages and retained the most effective one. We also adjusted the additional control points to add more curvature to the pressure side curve, in an

ISSN 2616-7433 Vol. 2, Issue 12: 116-122, DOI: 10.25236/FSST.2020.021217

attempt to increase the pressure above it. This improved the lift-drag ratio to 58. Finally, the leading-edge shape was modified (drooped) and its radius was reduced to lower the impact drag of approaching airflow. Several leading-edge radii were tested and finally the best performing radius of 2.5 mm was adopted. This improved the lift-drag ratio to 62. The final airfoil generated 497 Newtons of downforce per unit width at the expense of only of 8.7 Newtons of drag per unit width. The flow field of this airfoil is shown in Fig. 8. Due to a combination of the many refined geometric characteristics, this airfoil generated a pronounced and extended low-pressure zone under the suction side, as well as a large high-pressure zone above the pressure side; the result of these pressure zones is a large amount of overall downforce. The flow over the airfoil was nearly entirely laminar with very little separation or boundary layer transition, which minimized the viscous drag. Finally, the airfoil has an ideal leading-edge profile that minimizes the impact drag of approaching free stream airflow.

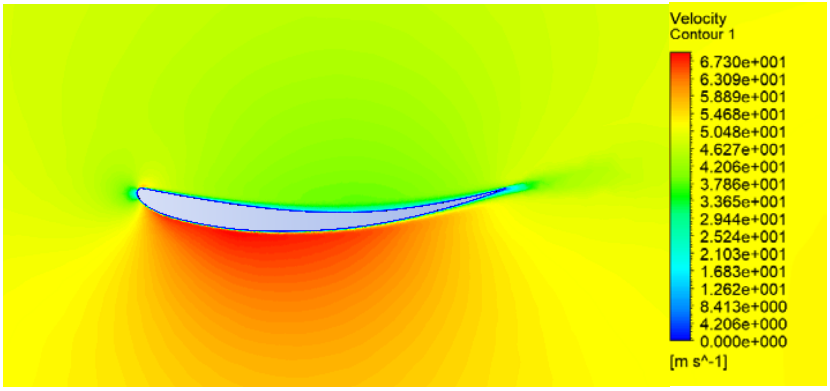

Fig.8 Velocity Contour of Final Airfoil

4. Discussion

Through test studies and optimization, we obtained an inverted airfoil with a high lift-drag ratio of 62. This inverted airfoil generated a large amount of lift at the expense of little drag. In theory, it can be extruded along the Z direction to obtain a full F1 rear wing that would help the car attain a good balance between cornering speed and straight-line speed, enhancing its overall performance. The strength and reliability of this study lie in its control-of-variables methodology, rigorous comparative analyses of the results, and the large number of airfoils tested. Distinct and highly consistent trends were discovered which we capitalized on to produce a genuinely effective design concept. However, there are also many limitations to our study. We have made many simplifications in the geometry modelling process and we only tested representative values of the independent variables instead a considering a continuous spectrum of values. As a result, our design did not reach the exact optimal performance under the given conditions (constant chord length of 35 cm and free stream air speed of 50 m/s). Indeed, more detailed studies will be conducted in the future to further refine this airfoil prototype. Another limitation of our study is that we only simulated a steady-state performance of the airfoil under a single speed, the average speed of F1 cars, whereas in reality, Formula One cars operate in a broad range of speeds, often accelerating and decelerating rapidly. Further investigation will focus on confirming whether the high lift-drag ratio of our airfoil design can be maintained across different speeds and during the transient state of rapid acceleration and other complex conditions experienced by Formula One cars.

5. Conclusion

In this work, we designed through comparative numerical simulation a F1 rear wing airfoil prototype that has a very high lift-drag ratio and a potential to be effectively applied to motorsports. This airfoil concept also has the potential to be applied to high-performance road cars, or even regular cars and SUVs because the aerodynamic downforce it generates can enhance the handling of all cars and provide crucial grip in bad weather conditions such as rainy and snowy days, improving drivers' safety. Moreover, its low-drag nature enables it to contribute to safety without sacrificing fuel economy----a desirable trait in the fuel-deficient 21st century. However, this airfoil should only be regarded as a prototype as many further simulations and experiments must be conducted before it can be put into use.

ISSN 2616-7433 Vol. 2, Issue 12: 116-122, DOI: 10.25236/FSST.2020.021217

References

[1] Dj.Kamari, M.Tadjfar, A.Madadi (2018). Optimization of SD7003 airfoil performance using TBL and CBL at low Reynolds numbers, Aerospace Science and Technology, no.79, pp.199-211.
[2] DENG Lei, QIAO Zhi-de, YANG Xu-dong (2011). Multi-point/objective optimization design of high lift-drag ratio for NLF airfoils, ATCA AERODYNAMICA SIICA, vol.29, no.3, pp.330-335.
[3] Talluri Srinivasa Rao, Trilochan Mahapatraa Sai, et al (2018). Enhancement of Lift-Drag characteristics of NACA 0012, Materials Today Proceedings, vol.5, no.2, pp.5328-5337.
[4] Liu Zhou, Zhu Ziqiang, Fu Hongyan (2004). Design of Airfoil with High Ratio of Lift over Drag, ATCA AERODYNAMICA SINICA, vol.22, no.4, pp. 410-415.
[5] Joseph Katz (2006). New Directions in Race Car Aerodynamics, 2nd Edition, Bentley Publishers.
[6] Yu Kai-nan, Xie Shi-bin (2018). Rear Wing Design and Optimization for Formula SAE car based on CFD, Journal of Mechanical & Electrical Engineering, vol.35, no.1, pp.16-21.